Fe and V Substituted Li_2MnSiO_4/C as Potential Cathode Material for Li-ion Batteries

Nils Wagner[a], Antoine Dalod[a], Ann -Mari Svensson[a] and Fride Vullum-Bruer[a]

[a]*Department of Materials Science and Engineering, Norwegian University of Science and Technology,*
7491 Trondheim, Norway

Lithium transition-metal silicate materials are promising candidates for next generation Li-ion batteries since they allow Li extraction/insertion beyond one Li ion per formula unit. They consist of cheap, non-toxic and abundant elements. Here we focus on the synthesis and electrochemical performance of Fe and V substituted Li_2MnSiO_4. Cations were substituted to overcome poor stability of the undoped compound and increase conductivity, thus expected to increase the electrochemical performance. Up to 20 mole % Fe and 5 mole % V were incorporated into orthorhombic $Pmn2_1$ Li_2MnSiO_4 while keeping a high phase purity and the desired porous nano-sized structure. For materials with 20 mole % Fe substitution, the reversible Li intercalation capacity during slow cycling (C/33) was increased from 0.63 Li per formula unit for the undoped to 0.81 for the doped sample. A 5 mole % V substitution increased the reversible Li capacity from 0.65 Li per formula unit to 0.73.

Introduction

Since Nyten *et al.* [1] reported Li_2FeSiO_4 as a new Li-battery cathode material in 2005, transition metal ortho-silicates came into focus as potential cathode materials for next generation Li-ion batteries [1, 2, 3]. Transition metal ortho-silicates, where the transition metal is Fe or Mn are environmentally benign. In theory Li_2MnSiO_4 allows the reversible exchange of up to two Li per formula unit, offering a theoretical capacity of 333 $mAhg^{-1}$ [2, 3]. Dominko *et al.* reported on the synthesis of Li_2FeSiO_4 (LFS) and Li_2MnSiO_4 (LMS) and found the major drawback of the transition metal ortho-silicates to be the low electronic conductivity, which in the case of LMS is about $3 * 10^{-14}$ Scm^{-1} at 60 °C [4, 5]. Furthermore, LMS suffers from severe capacity fading which is believed to be caused by a Jahn-Teller distortion of the tetrahedrally coordinated [Ar] $3d^4$ ion Mn^{3+} during charging [6]. The Li diffusion coefficient in LMS is also reported to be rather poor, $3.4 * 10^{-18}$ cm^2s^{-1} [7]. Means to remedy this would be to reduce the mean diffusion length for the Li ions by nano-structuring combined with application of a conductive carbon coating [5, 8]. LMS has recently been synthesized by various wet chemical methods such as solution routes, sol-gel, Pechini and polyol methods. [7, 8, 9, 10, 11, 12, 13].

Here we try to manipulate the electrochemical performance and the stability of LMS by doping strategies. We report on an acidic, PVA assisted sol-gel method leading to

nano-sized LMS particles agglomerated in a porous manner. A carbon coating is applied by adding corn-starch prior to the final heat treatment. Up to 20 mole % Mn was substituted by Fe since LFS is reported to facilitate a stable exchange of up to 1 Li ion per formula unit [1, 5, 14]. Also, the redox couple Fe II/III is located at lower potentials and thus more easily accessible [5]. Previous research has often focused on the substitution of Fe by Mn in LFS [15, 16], but here we focus on the Mn-rich side in the LMS-LFS system.

Another interesting approach is the incorporation of V into lithium transition metal ortho-silicates. V offers various accessible oxidation states and is thus a promising ion in electrode materials for Li-ion batteries [17]. Recently, density functional theory calculations showed V substitution into LFS structurally stable up to 50 mole % [17]. Furthermore, an experimental study has reported a successful incorporation of 10 mole % V into LFS. The incorporation of V on either Fe or Si sites, with an increase in electrochemical performance when V is incorporated on a Si site compared to an undoped LFS sample were shown in the study [18]. A second study reported the successful incorporation of 5 mole % V into LFS but a decline in electrochemical properties, as well as phase separation at higher V substitution levels [19]. We demonstrate increased electrochemical response of LMS by incorporation of 5 mole % V. To our knowledge V substitution in LMS has never been demonstrated before.

Experimental

Synthesis

The materials synthesis was done according to a PVA assisted sol-gel method. A more detailed description of the synthesis is published elsewhere [13]. A 25 mL aqueous solution of 0.06 mole $LiNO_3$ (Alfa Aesar, 99%) and 0.03 mole $Mn(NO_3)_2 \cdot 4H_2O$ (Merck Emsure for analysis, > 98%) was set to pH 1.5 by the addition of HNO_3 (Sigma-Aldrich, ≥ 65% pro Analysi), before it was mixed with 0.03 mole tetraethyl orthosilicate (TEOS) (VWR, 99%) dissolved in 20 mL EtOH (VWR Prolabo, 100%). The solution for Fe or V substituted samples was prepared in the same manner. In Fe substituted samples the Mn precursor was substituted in a range of 5-20 mole % by $Fe(NO_3)_3 \cdot 9H_2O$ (Sigma-Aldrich, > 98%) while keeping the pH constant at 1.5.

5 mole % V was attempted on either Mn or Si site by partly substituting the Mn or Si precursor with 10 mL of an acidic NH_4VO_3 (Sigma-Aldrich puriss p.a. > 99.5%) solution keeping the total solution volume and the pH value constant. The solution containing stoichiometric ratio of cations was then left for gelation at 60 °C for 6 h. The resulting gels were aged for 72 h before being dried at 120 °C and calcined at 450 °C in 95% Ar 5% H_2 (Harmix) 5. Fe substituted samples and undoped LMS reference samples were then mixed with 25 wt. % corn-starch as carbon source and finally heat treated for 10 h at 625 °C in Harmix 5. V substituted samples and LMS reference samples were mixed with 40 wt. % corn-starch as carbon source and heat treated with the same temperature program. Finished carbon coated samples are denoted as undoped LMS/C and substituted LMS/C.

Characterization

Powder X-ray diffraction analysis was performed on a Bruker D 8 Focus and a D 8 Advance Da-Vinci, both equipped with a linear PSD detector working in Bragg–Brentano (Θ/2Θ) geometry. Scans were recorded from 2Θ = 15–70° with a step size of 0.013° and an integration time of 1.5 s under CuK_α radiation. Topas (Bruker AXS Version 4.2) was used for calculations of lattice parameters, full pattern refinements and quantification of secondary phases.

Porosity and surface area data were acquired by nitrogen adsorption on a Micrometrics TriStar 3000 gas adsorption analyzer at a temperature of -195.85 °C (liquid nitrogen). Samples were degased for 24 h prior to analysis. 54 and 40 points were measured for the adsorption and desorption isotherms, respectively. T-plot theory based on BET theory was applied for micropore area and the external surface area differentiation [20, 21].

Further morphology analysis was carried out by field emission scanning electron microscopy on a Zeiss Supra 55 VP microscope. The working distance was 10 mm and the acceleration voltage was set to 10 kV.

Electrodes were fabricated by tape casting of a slurry containing 85 wt. % Fe or V substituted LMS/C samples or undoped LMS/C reference, 10 wt. % Super P Li and 5 wt. % PVDF binder. Electrodes were assembled in CR 2016 coin cells using 1 M $LiPF_6$ (Sigma-Aldrich, ≥ 99.99%) dissolved in a 3:7 volume ratio of ethylene carbonate (Sigma-Aldrich, 99%) and diethyl carbonate (Sigma-Aldrich, ≥99%) as electrolyte. Li foil as negative electrode, separated by a Celgard 2400 film. Galvanostatic charge-discharge measurements were performed at 24 °C in a potential window between 1.5 V and 4.8 V on a Maccor 4200. The charge rate 1C was defined as a current density of 330 mAg^{-1} for simplicity.

Results and discussion

Phase analysis

The synthesis parameters of LMS/C were optimized in a previous study [13] and obtained compounds were indexed to the orthorhombic $Pmn2_1$ polymorph of LMS. Minor traces of secondary phases, namely Li_2SiO_3 and MnO, were present in all samples. Fig. 1 a) shows the phase fraction from Rietveld refinements of undoped LMS/C and 5, 10, 15 and 20 mole % Fe substituted LMS/C. Fe was in all cases incorporated into the structure and the amount of secondary phases decreases with increasing Fe content. The shown phase fractions refer to the crystalline content and thus disregard the amorphous carbon coating obtained from the corn-starch added during the synthesis. A previous study revealed that 25 wt. % corn-starch led to 9 wt. % carbon in the compound [13]. A full pattern refinement of a sample with 20 wt. % Fe substitution is given in fig 1 b). HKL reflections of the main phases and secondary phases are included. 20 mole % Fe substitution was the highest Fe concentration feasible with the synthesis parameters used in this study. Higher Fe substitution levels caused a too low pH value during the synthesis

and hindered a proper gelation of the sol. Fig. 1 b) also shows traces of elementary Fe in the sample.

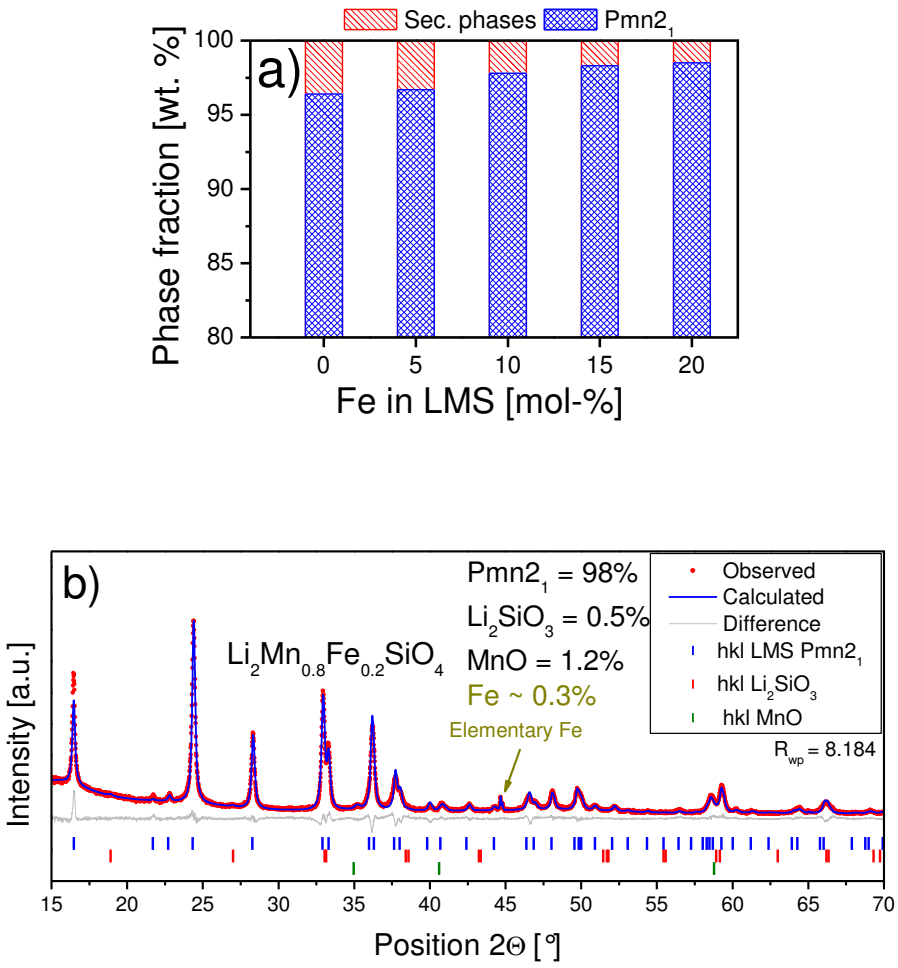

Fig. 1: a) Phase fraction for undoped and Fe substituted LMS/C samples. b) Powder XRD full pattern refinement of $Li_2Mn_{0.8}Fe_{0.2}SiO_4$

A further increase in the Fe concentration leads to an increased amount of elementary Fe in the compounds, since the Boudouard reaction resulting from the added carbon source and H_2 cause a severe reducing atmosphere during heat treatment. For higher Fe substitution levels the heat treatment atmosphere should be changed to Ar. Unit cell dimensions of LMS are in agreement with literature [4] and calculated to be a = 6.306 Å, b = 5.384 Å and c = 4.966 Å. Increasing Fe substitution leads to decreasing lattice constants which can be attributed to the difference in ionic radii of tetrahedrally coordinated Mn^{2+} and Fe^{2+} [22].

Vanadium incorporation was attempted on either the Mn^{2+} or the Si^{4+} site of LMS using a V^{5+} containing precursor. The addition of 25 or 30 wt. % corn-starch as carbon source was in both cases insufficient to form a carbon coating. Samples prepared showed a light grey body colour which is characteristic for samples with a low carbon content,

compared to black undoped and Fe substituted LMS/C samples. This might be caused by a consumption of the carbonizing agent during the reduction of V and/or reactions of ammonia with the carbonizing agent. Samples were finally successfully prepared using 40 wt. % corn-starch. Full pattern refinements of the nominal compositions $Li_2Mn_{0.95}V_{0.05}SiO_4$ and $Li_2MnSi_{0.95}V_{0.05}O_4$ are given in Fig. 2 a) and b) respectively. It should be mentioned that V can exist in multiple oxidation states from +II to +V where the existence of V^{3+} or V^{5+} would cause a deficiency of another cation in the compound for charge compensation.

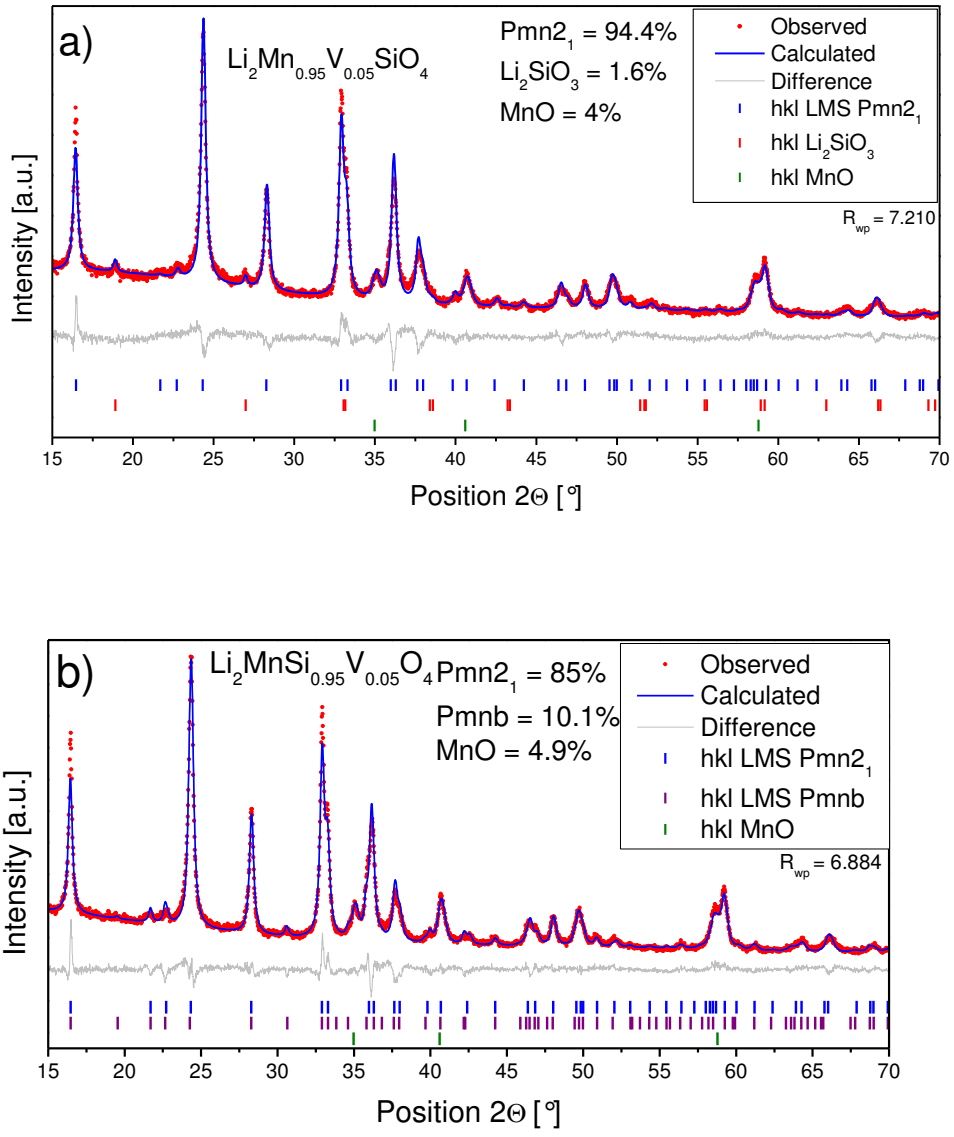

Fig. 2: Powder XRD full pattern refinements of the nominal compositions a) $Li_2Mn_{0.95}V_{0.05}SiO_4$ and b) $Li_2MnSi_{0.95}V_{0.05}O_4$

In both cases no V rich secondary phases appeared in the diffractograms. In the case of the intended composition $Li_2Mn_{0.95}V_{0.05}SiO_4$ the amount of MnO secondary phase is about 2 wt.% higher than in an undoped LMS/C sample. But it cannot be concluded if

this is a significant difference, since standard deviations of Rietveld phase fractions might be as large as 5%. In the diffractogram of the nominal composition $Li_2MnSi_{0.95}V_{0.05}O_4$ the amount of MnO is similar to $Li_2Mn_{0.95}V_{0.05}SiO_4$ while no Li rich secondary phase is detectable. Furthermore, about 10 wt. % of the orthorhombic Pmnb polymorph of LMS is present. The incorporation of 5 mole % V showed only a minor influence on the unit cell dimensions. However, the sample with the nominal composition $Li_2MnSi_{0.95}V_{0.05}O_4$ has a slight increase in the *c* lattice parameter from 4.967 to 4.973 Å. Rietveld refinements of numerous undoped LMS/C samples revealed that this increase is caused by the coexistence of LMS in $Pmn2_1$ and Pmnb space groups. Li *et al*. proposed a *c* parameter of 4.988 Å for LMS in $Pmn2_1$ [9]. However, the sample analyzed by Li *et al.* contained significant amounts of orthorhombic Pmnb in a $Pmn2_1$ matrix [9].

According to the Ellingham diagram of the V-O system the severe reducing atmosphere during heat treatment suggests that V^{5+} is reduced to V^{3+} [23]. The larger ionic radius of V^{3+} [22] would also cause V to occupy Mn sites rather than Si sites in LMS. The charge compensation could then be fulfilled by Mn deficiency according to the following defect equation:

$$[V]_{Mn}^{\bullet} = 2[Vac]_{Mn}'' \qquad [1]$$

Here, *[V]* is the concentration of vanadium, and *[Vac]* is the vacancy concentration.

V incorporation could also be compensated by Li deficiency and since Li is a very light element small changes in the Li content of LMS are not detectable by XRD. Finally, it needs to be mentioned that a definite answer to which site V occupies in LMS and in which oxidation state it occurs could not be determined. The V-O phase diagram is rather complex and shows a lot of different compounds with V in multivalent oxidation states between III and V [24].

The proposed defect equation is based on the XRD powder analysis, the increase in MnO secondary phase and abstinence of other secondary phases, and the severe reducing conditions during heat treatment.

Morphology

All powders consisted of porously agglomerated particles in the range 50-100 nm, and from SEM and nitrogen adsorption it is visible that all powders offer high accessible surface areas that can be penetrated by a liquid electrolyte.

In order to overcome the poor ionic conductivity of LMS, nano-sized particles with a high surface area accessible to the electrolyte are required. Fig. 3 shows the surface area of the different samples, a) for the Fe substitution series and b) for the V substitution. The surface area plots are divided into external area and micropore area, the latter being defined as porosity smaller than 2 nm and thus not accessible to solvated Li ions in the electrolyte [25]. The sum of external area and micropore area equals the BET surface area measured by nitrogen adsorption. In Fig. 3 b) $Li_2Mn_{0.95}V_{0.05}SiO_4$ is denoted as L(Mn95V5)S and $Li_2MnSi_{0.95}V_{0.05}O_4$ as LM(Si95V5).

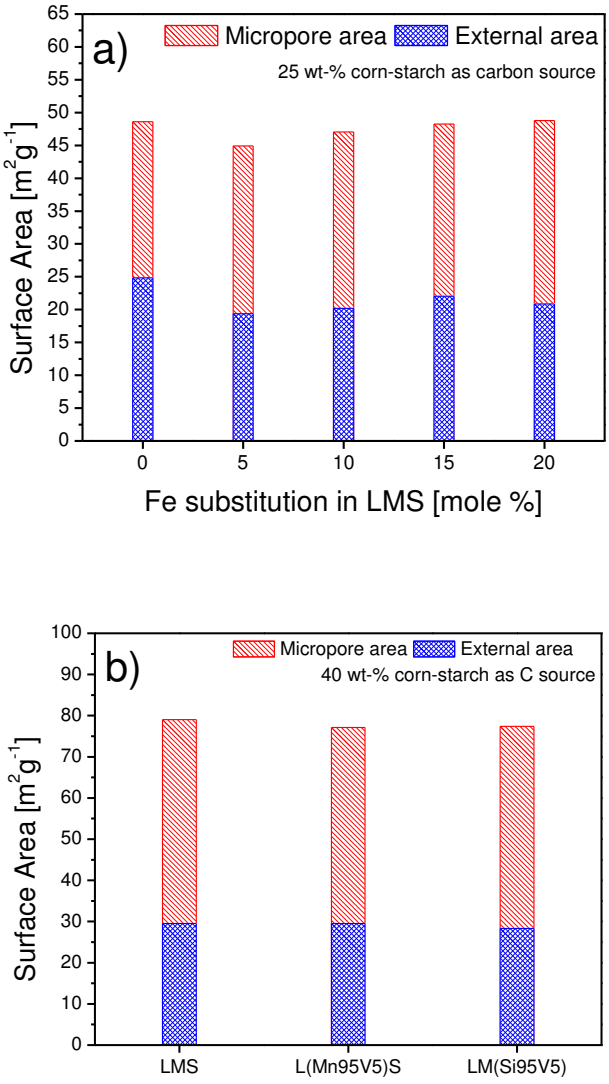

Fig. 3: BET surface area including micropore/external area separation: a) Fe substitution series b) V substitution

A previous study revealed that the microporosity can be attributed to the nature of the amorphous carbon coating [13]. Any amount of Fe substitution reduces the external surface area from approximately 25 m^2g^{-1} to 20 m^2g^{-1} while in the case of V substitution no difference was observed. External areas of the undoped and substituted samples were about 30 m^2g^{-1}. It needs to be mentioned that the corn-starch addition hinders particle growth and aggregation during heat treatment to a certain extent [13], hence undoped and substituted LMS/C samples shown in Fig. 3 b) offers an increased external surface area compared to those in Fig. 3 a). The increase in micropore area is caused by a higher carbon content due to the fact that 40 wt. % corn-starch was added with V substitution instead of 25 wt. with Fe substitution. SEM micrographs of a 10 mole % Fe substituted sample are given in Fig. 4.

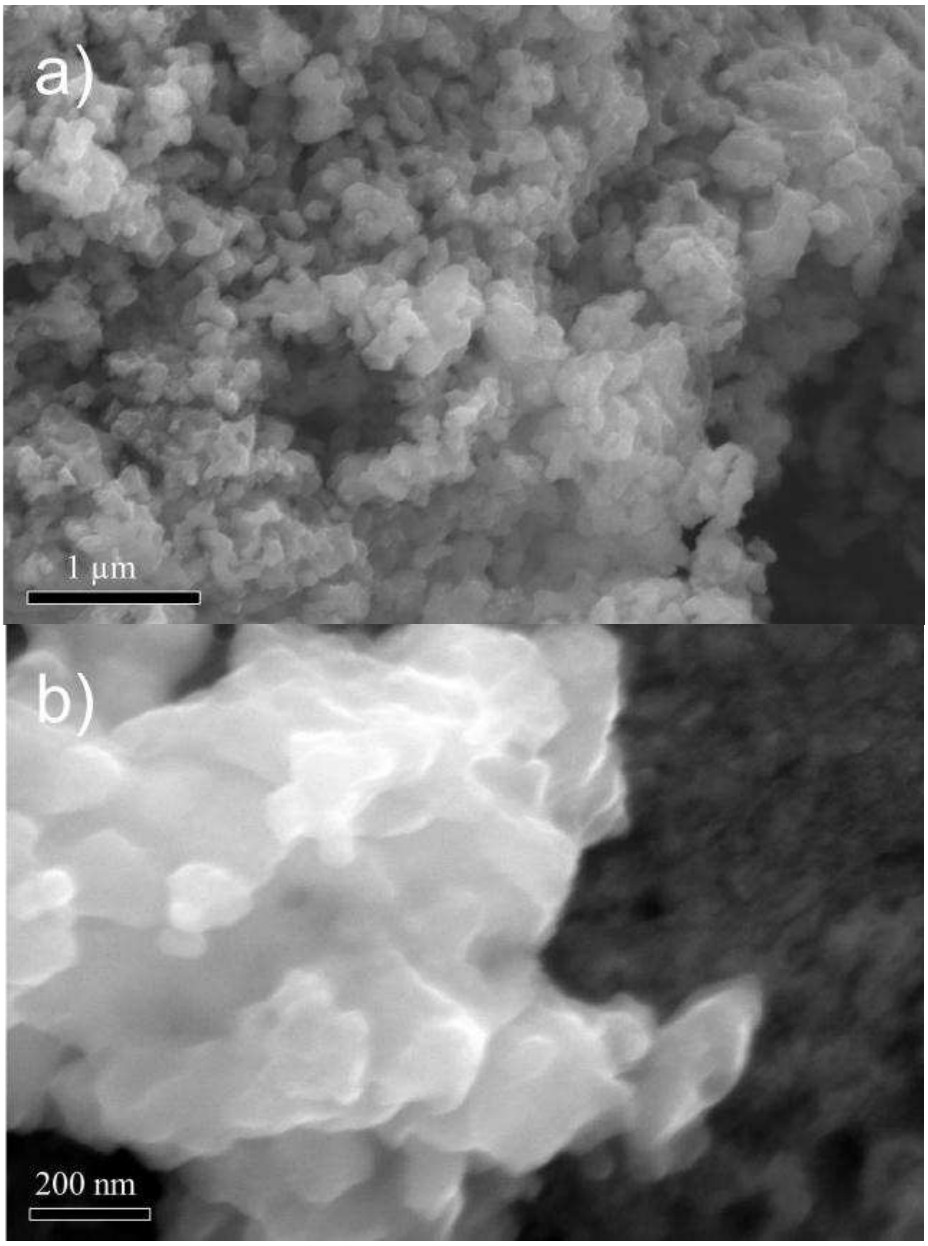

Fig. 4: SEM micrographs of a 10 mole % Fe substituted LMS/C sample: a) 20 k magnification b) 74 k magnification

Galvanostatic cycling

In order to investigate the effect of cation substitution in LMS/C, CR-2016 coin cells were fabricated with substituted LMS/C positive electrodes and the corresponding undoped LMS/C samples. Fig. 5 shows the galvanostatic cycling curves for Fe substituted samples. The first cycle of 10, 15 and 20 mole % Fe substituted samples against the undoped LMS/C at a current density of 10 mAg^{-1} (C/33) is given in Fig. 5 a). Fig. 5 b) shows the charge and discharge capacity of Fe substituted LMS/C samples for 12 cycles where the charge rate was C/33 in the initial three cycles, before it was increased to C/10 and then to C/4 for the three cycles at each charge rate and finally decreased again to C/33 for the last three cycles.

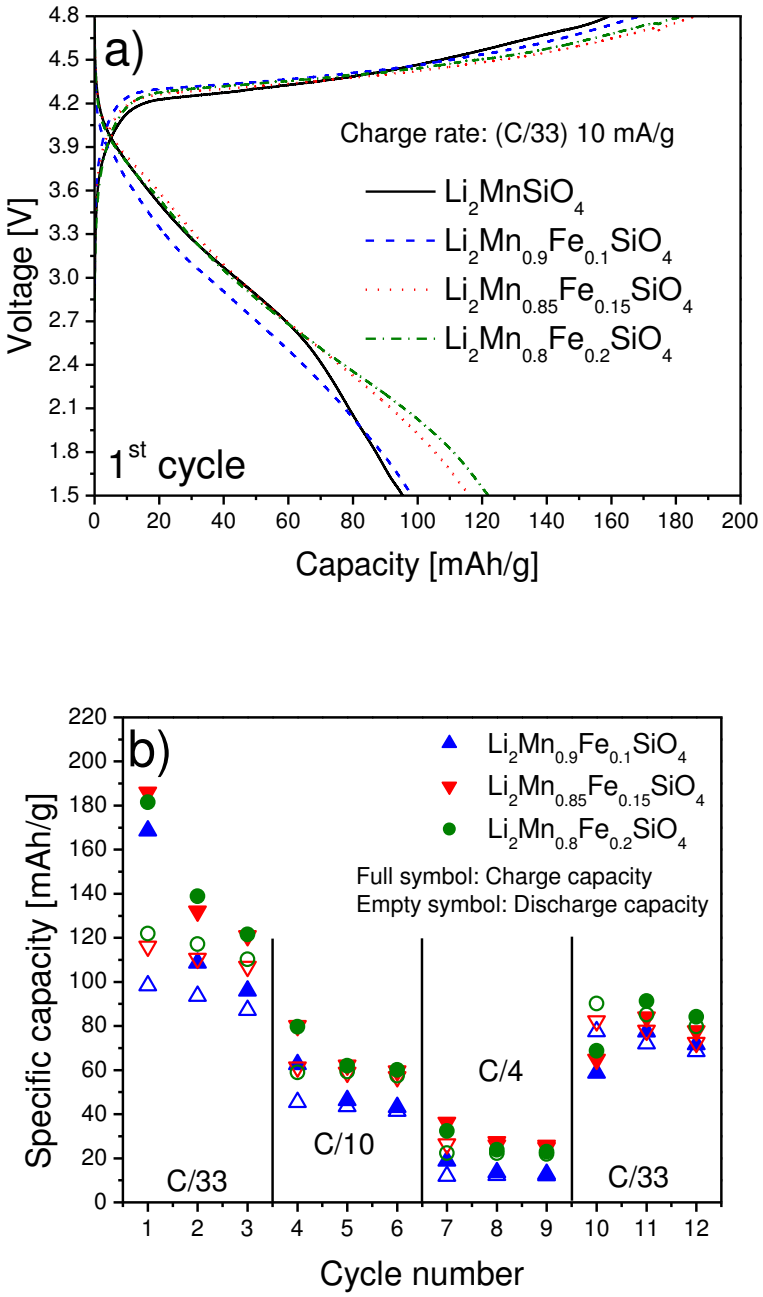

Fig. 5: Galvanostatic cycling of Fe substituted LMS/C (25 wt. % corn-starch as carbon source): a) First cycle of 10, 15 and 20 mole % Fe substituted LMS/C and an undoped LMS/C reference at C/33. b) Charge and discharge capacities of 10, 15 and 20 mole % Fe substituted LMS/C for 12 cycles at different charge rates

A clear increase in the first discharge capacity with increasing Fe content is visible in Fig. 5 a). The discharge capacity is increased from 95 $mAhg^{-1}$ for undoped LMS/C to 122 $mAhg^{-1}$ for the 20 mole % Fe substituted sample. Neglecting the carbon content (9 wt. %) these values correspond to approximately 0.63 and 0.81 Li per formula unit, respectively. This improvement could be attributed to a combination of improved structural stability

and higher Li diffusion and/or electronic conductivity. In addition, the irreversible capacity loss during the first cycle is reduced from 40 to 33%, which indicates that Fe substitution affects structural stability. Previously, an increase in rate capability with increasing carbon content in the samples have been demonstrated [13], hence poor rate capability shown in Fig. 5 b) is likely caused by low electronic conductivity of the samples. Despite this, an increase in performance even at higher rates is observed for higher Fe substitution levels, possibly due to improved Li diffusion rates, higher electronic conductivity, the at lower voltages situated Fe II/III redox couple or any combination of these factors. Overall capacity decay within the 12 cycles is still visible so the structural instability of LMS during cycling is still dominant even at 20 mole % Fe substitution.

Samples with 5 mole % V substitution were cycled in the same manner and results are illustrated in Fig 6. Fig. 6 a) shows the first cycle of both V substituted samples and an undoped LMS/C reference, also containing 40 wt. % corn-starch as carbon source to keep the approximate carbon content constant.

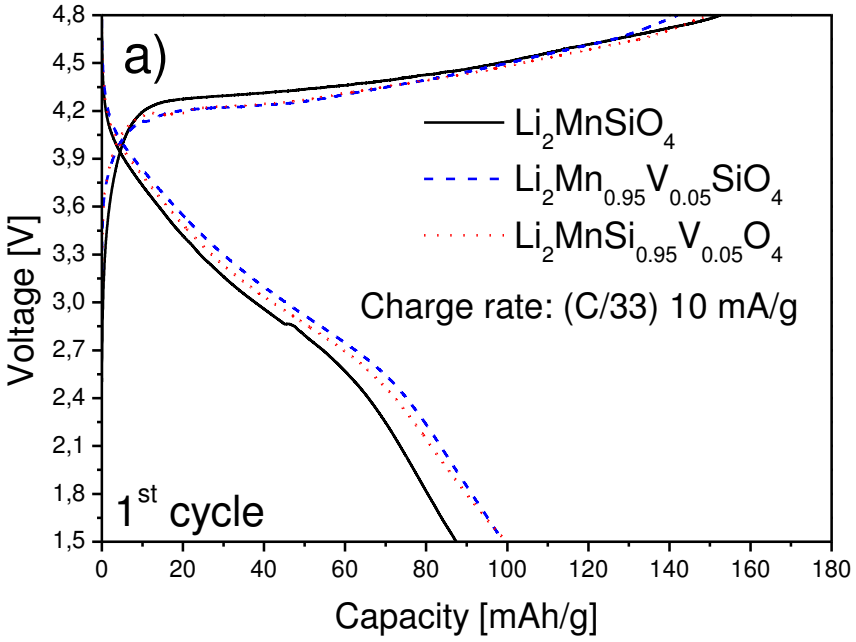

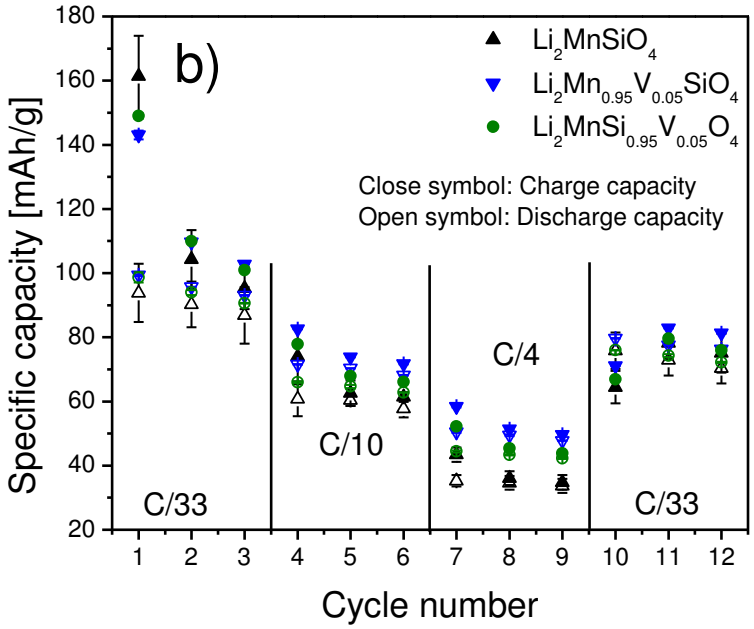

Fig. 6: Galvanostatic cycling of V substituted LMS/C (40 wt. % corn-starch as carbon source): a) First cycle of nominal compositions $Li_2Mn_{0.95}V_{0.05}SiO_4$/C and $Li_2MnSi_{0.95}V_{0.05}O_4$/C and an undoped LMS/C reference at C/33. b) Charge and discharge capacities for 12 cycles at different charge rates

Both V substituted samples behaved similarly, which suggests that V in both cases was incorporated on the same crystallographic site and exists in the same oxidation state. The first discharge capacity was in both cases, with values of 99 and 100 $mAhg^{-1}$, about 10% higher compared to the undoped sample with a discharge capacity of 88 $mAhg^{-1}$. This corresponds to an increase of the reversible Li exchange from 0.65 to 0.73 Li per formula unit. Furthermore, V substituted samples actually offered a lower charge capacity in the first cycle compared to the undoped material, and thus a reduction in the irreversible capacity loss of about 10%. The deintercalation potential is shifted to slightly lower potentials against Li/Li^+ and the intercalation potential is increased in potential against Li/Li^+. This is most probably caused by vacant sites in the structure which could influence the Li ion mobility. Whether or not V undergoes redox reactions in the structure and hence is electrochemically active cannot yet be concluded. Fig. 6 b) reveals that this increase in electrochemical performance is observed also at higher charge rates. V substituted samples showed discharge capacities of 45-50 mAhg $^{-1}$ at C/4 while undoped LMS/C only showed about 35 mAhg $^{-1}$, but the initial capacity could not be retained within 12 cycles.

Conclusions

Nano-sized LMS/C was successfully doped with up to 20 mole % Fe. Fe substituted LMS/C shows increased electrochemical performance. The reversible intercalation of Li in the first cycle was increased from about 0.63 Li per formula unit for an undoped LMS/C sample to 0.81 Li per formula unit for a 20 mole % Fe substituted sample during

cycling at 10 mAg^{-1}. Still, Fe substituted samples showed a poor rate capability and high capacity decay. Higher substitution levels are probably needed to overcome this behaviour. We also demonstrated the incorporation of 5 mole % V into LMS. It was intended to incorporate V either on a Mn site or on a Si site in LMS. Powder XRD data and the fact that the heat treatment is carried out under severe reducing conditions would indicate that V is present in the oxidation state III and would hence prefer a Mn site. V substitution enhanced the electrochemical performance and increased the reversible intercalation of Li from 0.65 to 0.73 Li per formula unit at 10 mAg^{-1}. Values of the intercalation and deintercalation potentials were also shifted, but it cannot be concluded if this is caused by the incorporation of vacant sites in the lattice or by redox activity of V.

Acknowledgements

The authors gratefully acknowledge the Research Council of Norway for funding of the SilicatBatt project (grant number: 216469/E20).

References

[1] Nyten A., Abouimrane A., Armand M., Gustafsson T., Thomas J. O., *Electrochemistry Communications,* **7,** 156 (2005).
[2] Saiful Islam M., Dominko R., Masquelier C., Sirisopanaporn C., Armstrong A. R., Bruce P. G., *J. Mater. Chem.*, **21,** 9811 (2011).
[3] B. L. Ellis, K. T. Lee, L. F. Nazar, *Chem. Mater.*, **22,** 691 (2010).
[4] Dominko R., Bele M., Gaberšček M., Meden A., Remškar M., Jamnik J., *Electrochemistry Communications,* **8,** 217 (2006).
[5] Dominko R., *J. Power Sources,* **184**(2), 462 (2008).
[6] Muraliganth T., Stroukoff K. R., Manthiram A., *Chem.Mater.* **22,** 5754 (2010).
[7] Świętosławski M., Molenda M., Furczo K., Dziembaj R., *J. Power Sources,***244,** 510 (2013).
[8] Gummow R. J., He Y., *J. Power Sources,* **253,** 315 (2014).
[9] Li Y. X., Gong Z. L., Yang Y., *J. Power Sources,* **174,** 528 (2007).
[10] Sun, D., Wang H., Ping D., Zhou N., Huang X., Tan S., Tang Y., *J. Power Sources,* **242,** 865 (2013).
[11] Devaraj S., Kuezma M., Ng C.T., Balaya P., *Electrochimica Acta,* **102,** 290 (2013).
[12] Liu W. G., Xu Y. H., Yang R., *Rare Metals,* **29,** 511 (2010).
[13] Wagner N., Svensson A-M., Vullum-Bruer F., Effect of carbon content and annealing atmosphere on phase purity and morphology of Li_2MnSiO_4 synthesized by a PVA assisted Sol-Gel method, *in preparation.*
[14] Nadherna M., Dominko R., Hanzel D., Reiter J., Gaberšček M., *J. Electrochem. Soc.*, **156,** A619**,** (2009).
[15] C. Deng C., Zhang S., Yang S. Y., *J. Alloys and Compounds,* **487,** L18 (2009).
[16] Guo H., Cao X., Li X., Li L., Li X., Wang Z., Peng W., Li Q., *Electrochimica Acta,* **55,** 8036 (2010).
[17] Li Y., Cheng X., Zhang Y., *J. Electrochem. Soc.,* **159**(2),A69 (2012).
[18] Hao H., Wang J., Liu J., Huang T, Yu A., *J. Power Sources,* **210,** 397 (2012).
[19] Yang H., Zhang Y., Cheng X., *J. Electrochemistry,* **19**(6), 565 (2013).

[20] Brunauer S., Emmett P. H., Teller E., *J.American Chemical Society,* **60,** 309 (1938).
[21] Harkins W. D., Jura G., *J. American Chemical Society,* **66,** 1366 (1944).
[22] Shannon R. D., *Acta Crystallographica,* **A 32,** 751 (1976).
[23] Yamaguchi I., Manabe T., *Thin Solid Films,* **366,** 294 (2000).
[24] Wriedt H. A., *Bulletin of Alloy Phase Diagrams,* **10**(3), 271 (1989).
[25] Zhou H., Einarsrud M-A., Vullum-Bruer F., *J Power Sources,* **235,** 234 (2013).